Journal of Sustainable Development of Energy, Water and Environment Systems

http://www.sdewes.org/jsdewes

Year 2025, Volume 13, Issue 2, 1130577

Original Research Article

Optimisation of 5th Generation District Heating and Cooling Networks for different Flow Configurations

Anna Dell'Isola [*1], ***Louis Hermans*** [1], ***Lieve Helsen*** [1,2]

[1]Department of Mechanical Engineering, KU Leuven, Belgium
e-mail: anna.dellisola@kuleuven.be
[1]Department of Mechanical Engineering, KU Leuven, Belgium
e-mail: louis.hermans@kuleuven.be
[1]Department of Mechanical Engineering, KU Leuven, Belgium
[2] EnergyVille, Thor Park, Waterschei, Belgium
e-mail: lieve.helsen@kuleuven.be

Cite as: Dell'Isola, A., Hermans, L., Helsen, L., Optimisation of 5th Generation District Heating and Cooling Networks through Different Flow Configurations, J.sustain. dev. energy water environ. syst., 13(2), 1130577, 2025, DOI: https://doi.org/10.13044/j.sdewes.d13.0577

ABSTRACT

Heating and cooling sectors are pivotal in the European Union's pursuit of climate neutrality by 2050. District heating and cooling networks, in particular the 5th generation, offer a valuable solution for reducing primary energy use and carbon dioxide emissions. This paper delves into the control optimisation of 5th generation district heating and cooling networks using white-box model predictive control techniques. The aim is to develop a nonlinear model predictive control approach for a 5th generation district heating and cooling network characterised by a directional medium flow and compare it to a non-directional medium flow network also controlled by nonlinear model predictive control. Physics-based models of building envelopes and hydraulics, developed in Modelica, are used. A model predictive control simulation is carried out to investigate the system's operation and make a comparison of both model predictive controlled 5th generation district heating and cooling networks. Despite being less flexible, the directional configuration achieves lower energy use and good thermal comfort by leveraging fluctuating network temperatures.

KEYWORDS

Fifth Generation District Heating and Cooling (5GDHC), Model Predictive Control (MPC), Modelica, Directional flow, Non-directional flow.

INTRODUCTION

In Europe, the heating and cooling demand accounts for more than 60% of the final energy use in the residential sector, yet renewables currently only supply a quarter of the EU's space heating needs [1]. District Heating and Cooling (DHC) networks, in particular the 5th Generation (5GDHC), represent a valuable solution for the reduction of primary energy use and both global and local emissions [2]. The primary objective of 5GDHC is to increase the share of residual and renewable energy sources (R^2ES) by lowering the supply temperature close to ground temperature ($T_s < 30$ °C), facilitating the exchange of low-quality thermal energy. While global warming is already progressing, the cooling of buildings is becoming more relevant in urban energy systems [3], which is another reason why 5th generation district heating and cooling (5GDHC) networks are gaining interest as they allow for simultaneous

* Corresponding author

heating and cooling through a bi-directional network. Heat pumps and/or chillers, in decentralized "active" substations, upgrade the low-exergy heat to the required quality, while a centralized balancing unit usually keeps the temperatures within a specified range [4].

However, the operation of these future-proof networks is not yet optimised, and the future enhancements of system performance through optimal integration and control of distributed heat and cold sources are needed, as highlighted in [4][5][6]. Meibodi *et al.* [7] introduced the use of the energy hub concept [8] for the design optimization of 5GDHC networks, but emphasized the necessity of new modelling approaches for the bidirectional energy flow in 5GDHC networks. Moreover, control strategies for 5GDHC networks vary significantly based on system configurations, temperature settings, and optimisation objectives, underscoring the need for advanced control strategies beyond rule-based controls [4].

Different classifications of 5GDHC networks exist, depending on the number of pipelines at different temperature levels and the direction of energy and medium flows. Buffa *et al.* [9] conducted a thorough survey on different 5GDHC networks in Europe and identified two main configurations of "prosumers" substations: i) Bidirectional energy – Non-Directional medium flow (BiND), ii) Bidirectional energy – Directional medium flow (BiD). In the most advanced solution with non-directional medium flow, the system is able to reject warm water (in active or free cooling mode) in the warm pipeline and cold water (in heating mode) in the cold pipeline. In this way, heat pumps will operate with higher COP thanks to optimal boundary conditions and both cooling and heating demands can be satisfied simultaneously. On the other hand, the directional medium flow configuration offers simpler hydraulics, but at the cost of lower performance in either heating or (not and) cooling mode. However, in the non-directional medium flow configurations, pump-to-pump interactions present a big challenge, as highlighted by Sommer *et al.* [10]. Large sizes of the decentralized pumps in the different substations strongly affect the mass flow rates through smaller proximal circulation pumps. These interactions may cause possible freezing problems in the heat pump due to lower mass flow rates or even reverse flows. For these reasons, a robust network control becomes crucial and challenging for the non-directional medium flow configuration, especially with increasing mass flow rates and extended networks.

Zanetti *et al.* [11] proposed an improved control strategy to reduce the energy use of pumps, highlighting the significant impact of pumping energy at low temperatures. Easiness, comfort, and affordability seem to dominate building owners' preferences for heating system choices in households, with increasing environmental awareness [12]. In this context, Taylor *et al.* [13] presented Model Predictive Control (MPC) as a particularly promising control strategy for 5GDHC networks, being able to predict evolving system states, taking into account the physical behaviour of the system, building thermal inertia, and weather forecasts. This allows for Demand Side Management (DSM) through system control, enhancing overall system performance by shifting heat demand or leveraging building inertia [14]. Different optimal control approaches have been presented in the literature by Frison *et al.* [15] and Wirtz *et al.* [16], with mixed-integer nonlinear program (MINLP) MPC for a bidirectional energy – non directional medium flow configuration, although these show simplified control-oriented models. Bünning *et al.* [5] developed an agent-based control strategy with network temperature optimisation, comparing different scenarios with different heating and cooling demands and boundary conditions. Sommer *et al.* [10] contributed to the state of the art by providing insights into the effect of different 5GDHC network configurations on total energy use. They compared a base-case double pipe network with a reservoir network through Modelica dynamic simulations. The operational and economic feasibility of bidirectional energy – directional medium flow configuration has been investigated by different studies in literature. Bilardo *et al.* [17] focused on modelling a low-temperature 5GDHC system, demonstrating its potential for enhanced efficiency and flexibility. An advanced thermo-hydraulic network model for 5GDHC systems with directional medium flow was also developed in [18], enhancing the accuracy of pressure drop and heat loss calculations by

incorporating temperature-dependent fluid viscosity and convection effects. However, both models rely on simplified demand profiles instead of detailed building simulations. Vivian *et al.* [19] explored smart control strategies for heat pumps in 5GDHC networks, yet their approach is constrained by post-processing control, limiting real-time adaptability. Saini *et al.* [20] conducted a techno-economic analysis, highlighting the economic viability of 5GDHC networks with a BiD configuration under various market conditions. However, the network and substations performance were evaluated in a co-simulation environment, increasing the complexity and neglecting key non-linearities in thermal and hydraulic behaviours. On the other hand, Penttinen *et al.* [14] highlighted the necessity to better understand the restrictions imposed by supply temperature reduction.

Despite these advancements, the existing studies often rely on demand profiles, simplified building models, or linear models, and rarely combine the strengths of detailed physics-based models, non-linearities, and direct optimisation without the need for post-processing controls. Hermans *et al.* [21] contributed filling this gap by developing a detailed controller model that includes nonlinearities for the specific BiND configuration.

Therefore, this study aims to develop a similarly featured controller for the directional medium flow configuration (BiD) for 5GDHC networks in order to assess its performance compared to the BiND configuration. The BiD configuration has a simpler hydraulic design which might eliminate the shortcomings of the non-directional medium flow configuration (BiND), guaranteeing more robust operation conditions. To compare both configurations (BiD and BiND) in a fair way, Model Predictive Control (MPC) is used as a strategy to minimise energy use, while providing thermal comfort. To enhance understanding of the impact of the different configurations on the 5GDHC system performance, dynamic simulations are performed using a virtual district. For the BiND configuration, a mixed-integer nonlinear programming (MINLP) MPC has already been developed and analysed by Hermans *et al.* [21]. For the BiD configuration, a new approach is developed and employed in this paper to solve the nonlinear Programming (NLP) MPC.

In addition, this paper assesses the impact of several key factors on the optimisation results, among them: the building thermal performance, the pumps energy use and the thermal comfort constraint imposed on the floor surface temperature. These factors are integrated into the MPC framework for the BiD configuration to provide a comprehensive analysis of their influence on system performance.

METHODS

This study introduces a novel nonlinear programming Model Predictive Control (MPC) formulation for the Bidirectional energy – Directional medium flow (BiD) configuration of a 5th Generation District Heating and Cooling (5GDHC) network. The performance of the BiD configuration is evaluated under two distinct Scenarios:

- Scenario A: This Scenario considers a district with poorly performing buildings. The objective is to minimize the total energy use of heat pumps and thermal discomfort, without imposing any constraints on the minimum floor temperature.
- Scenario B: This Scenario considers district with better-performing buildings. The goal is to minimize the total energy use of both heat pumps and pumps, as well as thermal discomfort, while also imposing a constraint on the minimum floor temperature.

For Scenario A, the BiD configuration, using the novel NLP MPC formulation, is compared to the non-directional medium flow (BiND) configuration, for which a Mixed-Integer Nonlinear Programming (MINLP) MPC formulation developed by Hermans *et al.* [21] is employed. Both optimisation problems for the two configurations are evaluated using the same cost function to ensure a fair comparison.

Scenario B is then compared to Scenario A to assess the impact of improved building performance, the inclusion of pumping power in the cost function, and the additional constraint on floor temperature.

For both scenarios, detailed physics-based models of building envelopes, thermal systems, and hydraulic components are developed in Modelica, an object-oriented, equation-based, acausal, multi-domain modelling language. These models are integrated into the MPC framework to create a high-fidelity controller model, ensuring effective exploitation of the system's flexibility.

The optimal control problems are formulated in TACO (Toolchain for Automated Control and Optimization), an in-house developed Modelica-based toolchain for nonlinear white-box MPC [22]. MPC simulations are conducted over an 8-month period (from January to August) to investigate and analyse the control behaviour of the two configurations. The energy use and thermal discomfort levels are then compared for the BiD and BiND configurations, as well as for the two MPC frameworks used for the BiD configuration.

Use case and model description

A small virtual 5GDHC network consisting of 4 residential buildings, 1 office building and a central balancing unit, serves as an example district to compare both configurations. The buildings are selected in order to simulate a typical Belgian district, with a variation in building quality (different UA values) and functions (residential and office). Linear two-zone white-box models for all buildings are created using the approach of De Jaeger *et al.* [23], with a day and night zone representative for the dwellings and a north and south zone for the office building.

Figure 1 shows the *UA*-value distribution of a typical Belgian district and the *UA*-value ranges of the buildings selected for the two Scenarios. In the transition from Scenario A to B, House 2 was replaced with a more energy-efficient building, still representative of the distribution but no longer at the extreme end. House 4 was also replaced, but the new building remains within the same *UA* range, however a building with improved window and roof transmittance was chosen to better accommodate low-temperature heating. As a result, two different buildings with distinct geometries were selected from the Belgian archetype buildings while maintaining consistency with the *UA*-value considerations. **Table 1** reports the main building parameters of the districts in both Scenarios. The heat power design value $\dot{Q}$ is calculated taking into account all heat loss terms (transmission, reheating, infiltration), using a setpoint of 21 °C and 18 °C for the day zone and the night zone respectively.

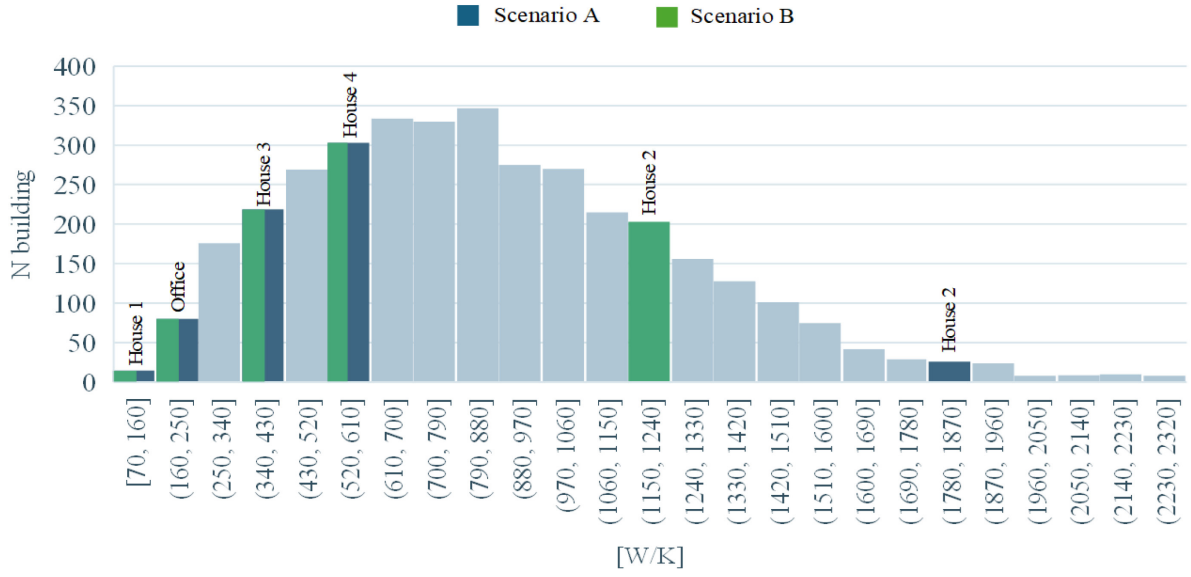

Figure 1. Typical Belgian district *UA*-value distribution [23]

Table 1. Summary of buildings specifications [23]

	House 1	House 2		House 3	House 4		Office
	A and B	A	B	A and B	A	B	A and B
A floor [m^2]	81	307	449	334	153	167	200
V [m^3]	269	1,093	1,394	1,027	517	565	600
$UA_{building}$ [W/K]	89	1,820	1224	392	550	542	173.1
U_{wall} [W/m^2/K]	0.145	2.359	2.335	0.48	2.100	2.27	0.333
$U_{ground\ floor}$ [W/m^2/K]	0.889	1.467	0.824	0.784	0.380	0.638	0.040
$U_{windows}$ [W/m^2/K]	1.631	5.86	3.534	2.055	3.028	1.909	1.400
U_{roof} [W/m^2/K]	0.345	3.107	0.572	0.336	1.400	0.605	0.349
n50 [1/h]	8	8	8	8	8	8	3
$\dot{\boldsymbol{Q}}$ design day zone [W]	2,835	28,325	23138	10,312	11,204	13,728	4,400
$\dot{\boldsymbol{Q}}$ design night zone [W]	2,664	29,699	23,267	10,073	9810	7,098	4,400

The considered central balancing unit then comprises of i) a large buffer tank (20 m^3), in order to dampen the seasonal temperature fluctuations in the network, ii) a large modulating air-source chiller (ASCH), and iii) a large modulating air-source heat pump (ASHP). The heat pump and chiller are necessary to maintain the buffer tank's temperature within the range of 3-16 °C. This network temperature range is set to avoid freezing and, at the same time, enable direct cooling, according to the average temperature adopted in 5GDHC networks [10], [24]. To keep new model development limited, the choice to use separate units (ASHP and ASCH) instead of a single reversible air-source heat pump was made without impacting the main findings. To model the HVAC components and the buildings the IDEAS Modelica Library is used for most parts [25]. The fundamental equations of these models can be found in the **APPENDIX** of this paper. However, as TACO requires that all model equations are continuous and twice differentiable, an in-house developed Modelica optimisation component library is used to model pumps, valves, and heat pumps.

The uninsulated district heating/cooling pipes (typically used in existing 5GDHC networks) are explicitly modelled by a single volume to account for the hydraulic limitations and heat losses of the network [24].

The considered emission system that provides both heating and cooling in each zone of the buildings is an embedded floor system controlled by two valves. The heating demand is satisfied by a modulating water-source heat pump (WSHP), while a heat exchanger (HEx) is used for direct cooling. The two configurations (BiD and BiND), compared in the present paper, mainly differ in the hydraulic scheme of the substation, presented in **Figure 2** and **Figure 3**. The BiD configuration is characterized by a centralized on-off pump, which determines a unique flow direction in the network. The flow can be directed through the direct-cooling heat exchanger or the WSHP depending on the positions of the three-way valves, which select the heating or cooling mode. In the more flexible BiND configuration, two

decentralized on-off pumps provide the fluid flow through the HEx or the WSHP depending on the mode selected by each prosumer.

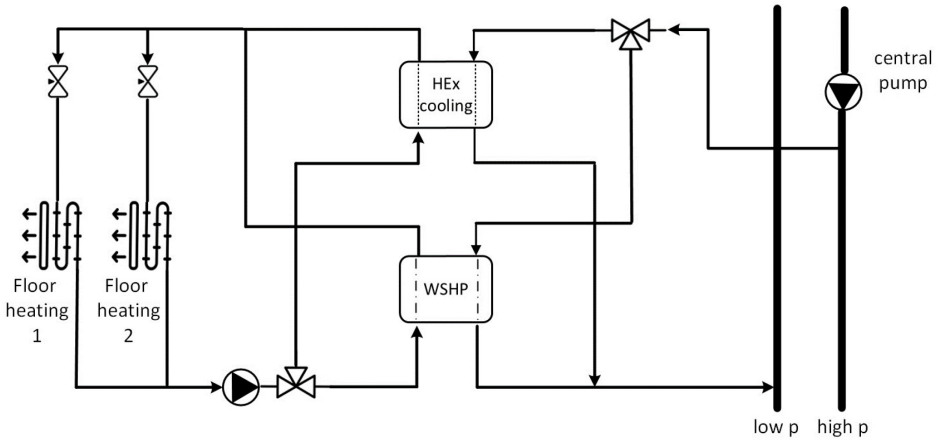

Figure 2. Simplified hydraulic scheme of bidirectional energy – directional medium flow (BiD) substation configuration

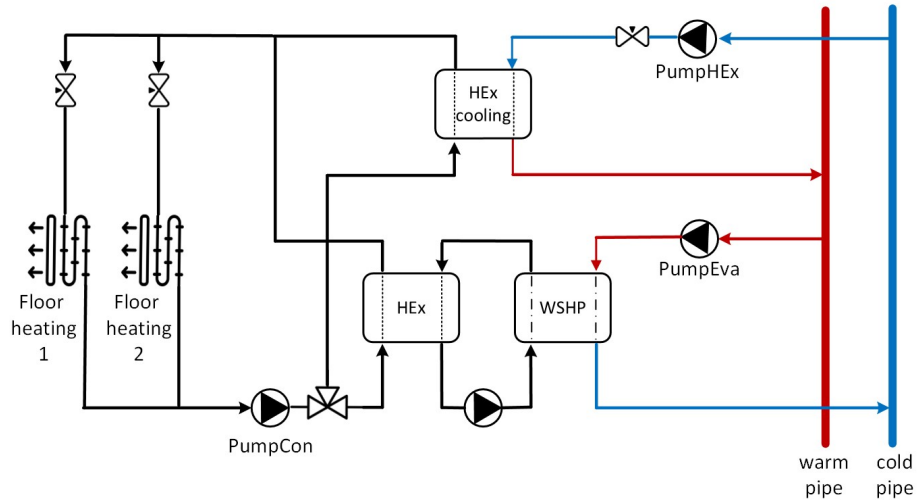

Figure 3. Simplified hydraulic scheme of bidirectional energy – non-directional medium flow (BiND) substation configuration [21]

The thermal system sizing and modelling is in line with the approach used in [21]. A nominal temperature difference of 3 K is considered across each substation, while a nominal temperature difference of 5 K is taken across the floor heating/cooling system. The total heat demand, $\dot{Q}_{\text{design}}$, of the connected buildings is then used for the heat pump and pipeline sizing.

The modelling approach used considers prescribed pressure head pumps, valves with linear opening characteristics, and a constant effectiveness (0.8) heat exchanger. The central buffer tank is modelled as a perfectly stratified two-layers tank, with two mixing volumes of each 10 m^3. The substation heat pumps (WSHP) and central heat pump (ASHP) coefficients of performance (COP) and the central chiller (ASCH) energy efficiency ratio (EER) take into account the temperatures dependency, according to eqs. (1a), (1b), (1c) respectively [26]:

$$\text{COP}_{\text{WSHP}} = 6.4 - 0.16\left(T_{\text{con,out}} - 29\right) + 0.1\left(T_{\text{eva,out}} - 11\right) \quad (1a)$$

$$\text{COP}_{\text{ASHP}} = 4.7 - 0.16\left(T_{\text{con,out}} - 20\right) + 0.1\left(T_{\text{eva,out}} - 6.98\right) \quad (1b)$$

$$\text{EER}_{\text{ASCH}} = 3.7 - 0.16\left(T_{\text{con,out}} - 20\right) + 0.1\left(T_{\text{eva,out}} - 6.98\right) \quad (1c)$$

where $T_{\text{con,out}}$ [°C] and $T_{\text{eva,out}}$ [°C] are respectively the condenser and evaporator outlet temperatures. The part-load limitations and efficiencies are not taken into account in this case.

Occupancy schedules and related temperature setpoints are used to assess the thermal comfort inside the buildings. Standard office hours spanning from 8 a.m. to 6 p.m. during weekdays are considered. In the residential buildings, the setpoint temperatures are between 21-23 °C and 18-25 °C for the day and night zone respectively, when people are present (which is outside the office hours), while between 15-27 °C when no one is present. No internal gains are considered for the residential occupants. The temperature ranges for the office building are set between 21-23 °C during the office hours and 15-27 °C when no people are present. 20 people are assumed to be present in the office and a fixed internal heat gain of 55 W/person is considered. The metabolic heat gains are set to 45 W latent heat production per person and 73 W sensible heat production per person [27]. IDEAS library's TMY-file (Typical Meteorological Year) for the Belgian region of Uccle is used for the ambient temperature and solar irradiation information.

Model predictive control formulation

Two optimisation problems are formulated, one for Scenario A and one for Scenario B, presented by eqs. (2a)-(2j) and eqs. (3a)-(3c) respectively. The optimal control problems are solved within an ideal MPC, where the physics-based simulation and controller model are the same. Perfect knowledge of the weather conditions is assumed within the prediction horizon Δt_{pr} of 3 days and a time step of 1 hour. In Scenario A, the problem is described by eqs. (2a) – (2j):

$$\min_{o(t)} \int_{t_i}^{t_i+\Delta t_{\text{pr}}} \left(J_{\text{el}}(t) + w_1(a^2+b^2) + \sum_{n=1}^{N_{\text{z}}} w_{2_n}(c_n^2+d_n^2) \right) dt \tag{2a}$$

$$s.t. \quad \frac{d\boldsymbol{x}(t)}{dt} = \boldsymbol{F}(\boldsymbol{x}(t), \boldsymbol{z}(t), \boldsymbol{o}(t), t) \tag{2b}$$

$$0 = \boldsymbol{H}(\boldsymbol{x}(t), \boldsymbol{z}(t), \boldsymbol{o}(t), t) \tag{2c}$$

$$x(t_0) = x_0 \tag{2d}$$

$$T_{\text{tank,min}} - T_{\text{cold,tank}}(t) \leq a \tag{2e}$$

$$T_{\text{warm,tank}}(t) - T_{\text{tank.max}} \leq b \tag{2f}$$

$$T_{\text{min},n}(t) - T_{\text{z},n}(t) \leq c_n, \qquad n = 1, \dots, N_{\text{z}} \tag{2g}$$

$$T_{\text{z},n}(t) - T_{\text{max},n}(t) \leq d_n, \qquad n = 1, \dots, N_{\text{z}} \tag{2h}$$

$$c_n, d_n \geq 0, \quad n = 1, \dots, N_{\text{z}} \tag{2i}$$

$$a, b \geq 0 \tag{2j}$$

The state variables are represented by the vector $\boldsymbol{x}(t)$, the optimisation variables by the vector $\boldsymbol{o}(t)$, and the remaining algebraic variables by the vector $\boldsymbol{z}(t)$. The main objective of the optimisation problem is to minimise the total energy use, while still guaranteeing thermal comfort inside the buildings. The objective integrand $J_{\text{el}}(t)$ in eq. (2a) takes into consideration the energy use of the decentralised heat pumps, central heat pump and central chiller. The soft

constraints on the semi-fluctuating network temperature (represented by the storage tank temperatures) and thermal discomfort in the building zones are implemented by eqs. (2e) and (2f), eqs. (2g) and (2h), respectively, by introducing the slack variables a, b and $c_{\mathrm{n}}, d_{\mathrm{n}}$. $T_{\mathrm{cold,tank}}, T_{\mathrm{warm,tank}}$ are the temperatures of the two mixing volumes, permitted to fluctuate into the range of $T_{\mathrm{tank.min}} - T_{\mathrm{tank.max}}$, $T_{\mathrm{z},n}(t)$ is the n^{th} zone temperature, $T_{\mathrm{max},n}, T_{\mathrm{min},n}$ are the maximum and minimum allowed temperatures in cooling and heating seasons in the n^{th} zone, and N_{z} is the total number of zones. The governing equations, represented by functions $\boldsymbol{F}$ and $\boldsymbol{H}$ in eqs. (2b) and (2c), describe the dynamic behaviour of the system for the controller model. Since these equations must always be satisfied, they are incorporated as equality constraints in the problem formulation.

To assess the effect of the refinements in Scenario B, the optimisation problem is adapted according to eqs. (3a), (3b), (3c):

$$\min_{o(t)} \int_{t_i}^{t_i+\Delta t_{pr}} \left(J_{\mathrm{el}}(t) + w_1(a^2 + b^2) + \sum_{n=1}^{N_z} w_2(c_n^2 + d_n^2) + w_2(e_n^2) \right) dt \tag{3a}$$

$$T_{\mathrm{em.min}} - T_{\mathrm{em,n}}(t) \leq e_n, \qquad n = 1, \dots, N_z \tag{3b}$$

$$e_n \geq 0, \quad n = 1, \dots, N_z \tag{3c}$$

In the second optimisation problem, the energy use of all heat pumps, chiller, circulation pumps and centralised pump is taken into account in the objective integrand $J_{\mathrm{el}}(t)$. Possible condensation problems in the embedded emission system are now avoided by using the additional soft constraint on the floor surface temperature in the n^{th} zone $T_{\mathrm{em},n}$, which should be above a minimum temperature $T_{\mathrm{em.min}}$ of 17 °C, as specified by [28].

The thermal penalisations for the BiD configuration are scaled with respect to the energy use in eq. (2a) and eq. (3a) by a weighting factor w_1 of 100 W/°C^2 for the network temperature constraint and w_2 of 5000 W/°C^2 for the thermal discomfort and floor surface temperature constraints. These weighting factors are determined through trial-and-error and kept constant within the two Scenarios, aiming for a well-conditioned optimisation problem and small convergence time.

In the BiD configuration, the optimisation control variables are the modulation of all heat pumps and the central chiller, the opening of the two-way floor heating valves, and selection valves. The latter are controlled optimising a parameter u between $[-1,1]$. A smooth approximation of the ramp function of u is used as the valve opening input to ensure it is twice differentiable. This method allows the selection valve for active heating to open when u is positive, while the valve controlling flow through the direct cooling heat exchanger (HEx) opens when u is negative. In the BiND configuration, similarly the modulation of all heat pumps and the central chiller, the prescribed pressure head of the underfloor heating/cooling circulation pumps, and the opening of the two-way valves inside the buildings (floor heating valves, selection valve) are optimised. The two-step MINLP-based MPC method used in this configuration is described in [21]. All equations and variables from the Modelica controller model are immediately inferred by TACO. These equations are then solved by a derivative-based NLP solver [22].

RESULTS

This section presents the results of the 8-month MPC simulation for the two configurations and settings analysed. In the first step, the directional and non-directional configurations are compared. Table 2 summarises the main results for Scenario A, in terms of electricity use of

the decentralised heat pumps and central units (ASHP and ASCH), and thermal discomfort. Based on the ASHRAE standard 55 [28] and the ISO7730 standard [29], the need for thermal comfort in the Belgian climate can be converted into a requirement on the operative temperature. Therefore, according to [30], thermal discomfort can be measured in Kelvin-hours.

Table 2. Electric energy use [kWh] and thermal discomfort [Kh] results summary for Scenario A (BiD: bidirectional-energy – directional medium flow configuration, BiND: bidirectional-energy – non-directional medium flow configuration)

Component	Configuration	Thermal Discomfort [Kh]	Heat Pump Electricity Use [kWh]
House 1	BiD	16	496
	BiND	7	516
House 2	BiD	2,192	15,399
	BiND	176	15,251
House 3	BiD	68	2,308
	BiND	28	2,325
House 4	BiD	104	4,111
	BiND	34	3,495
Office	BiD	214	512
	BiND	131	841
Balancing Unit	BiD		15,328
	BiND		18,565
Total	BiD		38,154
	BiND		40,994

The BiND configuration presents a total heat pump electricity use of 41 MWh, while the BiD configuration outperforms it with 38 MWh over the 8-month period. A similar approach as the one used in [21] is adopted for the comparison of the seasonal performance factor (SPF) in the two configurations, evaluating the total benefit in each building, in terms of heat provided in winter period $\dot{Q}_{\mathrm{WSHP,con},n}$ and extracted in summer period $\left|\dot{Q}_{\mathrm{HEx},n}\right|$, versus the total heat pump electric energy use over the simulation period E_{tot} , eq. (4):

$$\mathrm{SPF} = \frac{\sum_1^{Nb}\left|\dot{Q}_{\mathrm{HEx},n}\right| + \dot{Q}_{\mathrm{WSHP,con},n}}{E_{\mathrm{tot}}} \tag{4}$$

Both configurations show an SPF value of 3.34. This indicates that the electricity use reduction reflects into a lower thermal benefit in the directional medium flow configuration compared to the non-directional one, as expected from the observed thermal discomfort inside the buildings. This is clearly noticeable in House 2, where a particularly high level of thermal discomfort is balanced with limited energy use, due to the poor performance of the building envelope. The average COPs and EER of the different components in the buildings (Houses and Office) and in the central balancing unit are compared in **Figure 4**. It can be observed that the average COPs of the decentralised and centralised heat pumps in the BiND configuration are higher, leading to lower thermal discomfort for similar energy use. On the other hand, the efficiency of the centralised chiller is higher in the BiD configuration, with significantly lower energy use.

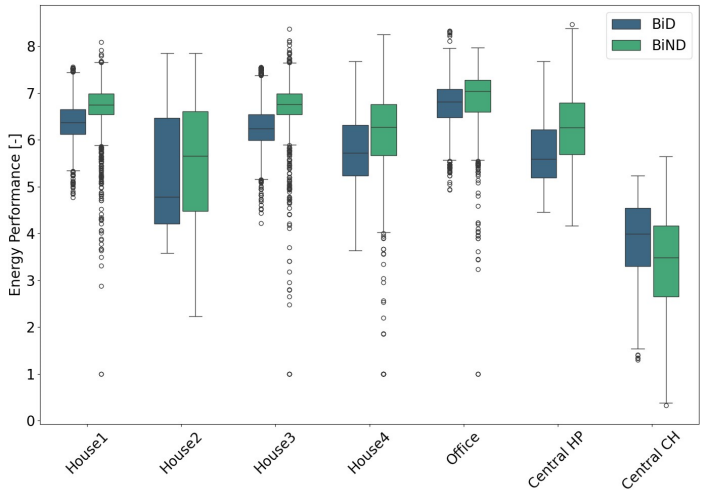

Figure 4. Energy performance (COP or EER) comparison of the different components (decentralised heat pumps, centralised heat pump and chiller) in the two configurations in Scenario A

The difference between the two configurations mainly occurs due to different supply temperatures to the heat pumps. **Figure 5** shows the daily average network temperatures as the daily average temperatures of the buffer tank for the BiD configuration and BiND configuration. The supply temperature is represented by the average temperature of mixing volume 1 (i.e. upper part of the stratified tank), while the return temperature corresponds to the one of mixing volume 2 (i.e. lower part of the stratified tank). It can be observed that the BiND configuration, compared to the BiD configuration, allows for higher average network temperatures on the primary side during the heating season, due to its enhanced flexibility and self-balanced network. Indeed, the excess heat resulting from high internal heat gains in the office is injected directly in the warm pipe, enabling a lower energy use from the central ASHP. This results in an average supply temperature for the period January-March of 10 °C for the BiND configuration, versus 7 °C for the BiD configuration. Based on eq. (1a), the temperature difference at the primary side (WSHP evaporator side) between the two configurations can lead on average to a COP difference of 0.3 in the decentralized units for the same condenser outlet temperature. Conversely, an average supply temperature for the period June-August of 9 °C is achieved for the BiND configuration compared to a higher average temperature of 13 °C in the BiD configuration. The lower network temperatures in the cooling season result in a decreased EER of the central chiller (ASCH) for the BiND configuration.

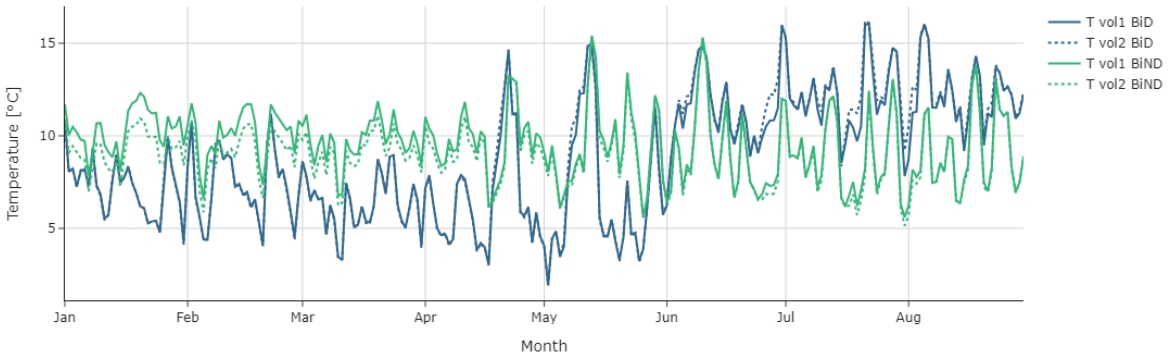

Figure 5. Comparison of the daily average buffer tank temperatures (T vol1- supply temperature, T vol2 - return temperature)

As a consequence, higher supply temperatures can be reached on the secondary side at the condenser outlet in the substations for the BiND configuration. Thereby, thermal discomfort in the buildings can be reduced, while maintaining acceptable COPs with an overall heat pump

electricity use of 22.4 MWh in the substations. In contrast, the BiD configuration, compared to the more advanced BiND configuration, results in lower indoor thermal comfort for a similar energy use of 22.8 MWh in the substations. However, the higher EER in the BiD configuration results in lower electricity use of the central chiller, reducing it to 1.4 MWh compared to 5.5 MWh in the BiND configuration, ultimately leading to lower overall energy use.

In the first district analysed in Scenario A, Houses 2 and 4 exhibit a poorly performing building envelope compared to the other residential buildings. This results in higher thermal discomfort in these buildings and elevated floor surface temperatures to achieve the desired temperature setpoint, often exceeding the maximum allowable limit of 31 °C during the heating season [28]. Consequently, it can be concluded that these buildings are not suitable for a 5GDHC network.

To investigate the effect of improving the building envelope quality, adding pump energy to the objective and including a floor surface temperature constraint, Scenario A is compared to Scenario B for the bidirectional energy – directional medium flow (BiD) configuration. The main results in terms of total electric energy use and thermal discomfort are reported in Table 3 for both Scenarios. The district of better-performing buildings in Scenario B achieves lower energy use while maintaining comparable average COPs and ensuring good thermal comfort inside the houses. This results in an overall reduction of energy use of 43%. The optimal solution in Scenario B leads in general to low thermal discomfort in the unchanged Houses 1 and 3, for a similar heat pump electricity use compared to Scenario A. The refined Houses 2 and 4 show thermal discomfort values below 101 Kh/zone, with consistent reduction in the heat pump electricity use, particularly for House 2 from 15.4 MWh in Scenario A to 7.2 MWh in Scenario B. Additionally, it is observed that the circulation pump electricity use in Scenario B is significantly reduced in all buildings and in the central circulation pump, with a total reduction of 76%. This is achieved thanks to lower mass flow rates at both the primary and secondary side of the substations. Figure 6 shows the mass flow rates ranges for the two Scenarios A and B in the substations at the secondary side and in the network.

Table 3. Electric energy use [kWh] and thermal discomfort [Kh] results summary for BiD configuration

Component	Scenario	Thermal Discomfort [Kh]	Average COP [EER] [-]	Heat Pump Electricity Use [kWh]	Circulation Pump Electricity Use [kWh]	Total Electricity Use [kWh]
House 1	A	16	6.4	496	274	770
	B	34	5.8	404	29	433
House 2	A	2,192	5.3	15,399	750	16,149
	B	202	5.7	7,234	380	7,614
House 3	A	68	6.3	2,308	592	2,899
	B	65	6.0	2,322	139	2,461
House 4	A	104	5.8	4,111	604	4,715
	B	92	5.6	3,842	205	4,047
Office	A	214	6.7	512	474	986
	B	1,010	6.2	576	188	765
Balancing Unit	A		5.7 [3.8]	15,328		15,328
	B		6.0 [4.4]	10,029		10,029
Network	A				5,728	5,728
	B				1,028	1,028
Total	A			38,154	8,420	46,574
	B			24,408	1,970	26,377

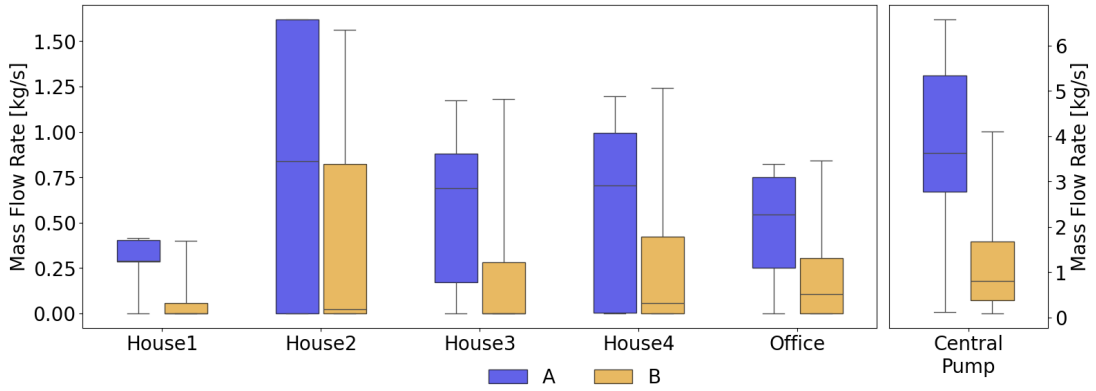

Figure 6. Mass flow rates comparison for Scenario A and B for BiD configuration

Thermal comfort in the heating season in the buildings is ensured by higher average supply temperatures at the condenser outlet in the Scenario B. **Figure 7** compares the distributions of the temperatures at condenser outlet in the decentralised WSHPs. The average temperatures at the condenser outlet for the unchanged buildings (House 1, 3 and Office) are clearly higher in Scenario B, with the inclusion of the pumping power into the objective function. This result allows for lower mass flow rates, minimizing the circulation pumping power, still meeting the thermal demand of the different buildings in the heating season. For House 2 and 4 it is observed that the better performing buildings in Scenario B show acceptable supply temperature ranges compared to Scenario A, with a significant reduction for House 2.

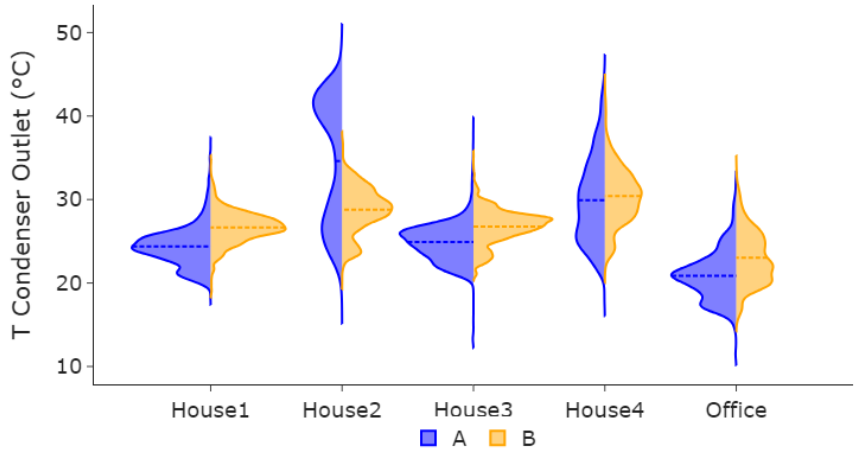

Figure 7. Condenser outlet temperature distributions for Scenario A and B for BiD configuration

However, the total thermal discomfort in the cooling season in the office has increased in Scenario B, resulting in a total thermal discomfort of 1010 Kh. This is a result of the extra constraint on the minimum floor surface temperature (to avoid condensation) in the cost function of the optimisation problem. **Figure 8** shows the evolution of the temperatures in the north and south zone of the office building in the period 20-25 August for Scenario A and Scenario B. It is observed that the temperatures in Scenario B are exceeding the upper setpoint temperature of 23 °C when there are occupants. In this case, the significant heat gains from occupancy and large windows in the office are no longer adequately compensated because of the limited cooling potential with a minimum allowed floor surface temperature of 17 °C.

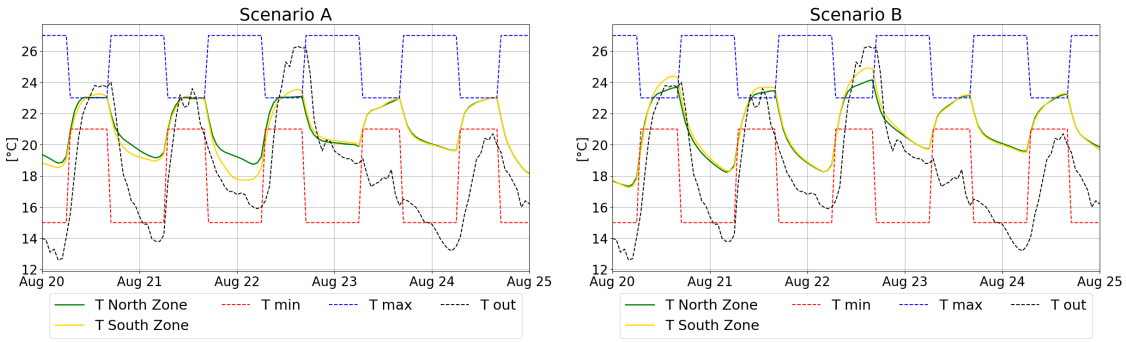

Figure 8. Evolution of the temperature in the north and south zone of the office building in summer period for BiD configuration

CONCLUSIONS

This paper presents a comparison between a novel NLP-based MPC control strategy for a bidirectional energy – directional medium flow (BiD) configuration, and an existing MINLP-based MPC control for a bidirectional energy – non-directional medium flow (BiND) configuration. Both strategies are applied to a small, virtual 5GDHC network, incorporating the non-linear dynamics of the hydraulic system and directly determining the optimal control inputs to realistic systems. An 8-month MPC simulation is conducted for both approaches in Scenario A, minimizing the total energy use of heat pumps and thermal discomfort in a base-case district with low performing buildings. Additionally, the study evaluates the impact of building thermal performance, pumps energy use and floor surface temperature constraint for the BiD configuration in Scenario B. It can be concluded that the two configurations show similar performances with a seasonal performance factor (SPF) of 3.34 in both configurations. However, the BiND configuration demonstrates an advantage by leveraging system flexibility to achieve higher thermal comfort while reducing energy use. The full potential of the BiND configuration is only partially exploited in this use case, due to a heating dominated cluster of buildings. A more diversified range of building functions could lead to higher COPs in the decentralised systems and to lower electric energy consumptions in the balancing units. Conversely, the BiD configuration maintains low energy use with 38 MWh, outperforming the BiND configuration with 41 MWh in Scenario A. However, the BiD configuration results to be infeasible if low performing building are included in the district, reaching high thermal discomfort values of 1096 Kh/zone in the badly performing House 2.

Moreover, the BiD configuration in Scenario B reaches effective thermal comfort values in the residential buildings, while achieving an overall reduction of energy use of 43% compared to Scenario A. However, the constraints on the floor surface temperature limit the heating/cooling capacity of the thermal system. This limitation results in higher thermal discomfort particularly during the cooling season for well-insulated and high-occupancy buildings. Additionally, the pumping power required is significantly reduced from 8.4 MWh to 1.9 MWh, when it is incorporated into the optimisation objective.

ACKNOWLEDGMENT

Funded by the European Union

The authors would like to thank Filip Jorissen (Builtwins) for all his TACO developments, and acknowledge the funding by the European Union through the HeriTACE (grant number 101138672) and SEEDS (grant number 101138211) project under the Horizon Europe Programme. Views and opinions expressed are however those of the author(s) only and do not

necessarily reflect those of the European Union or HADEA. Neither the European Union nor the granting authority can be held responsible for them.

NOMENCLATURE

A	heat transfer area	[m^2]
a	slack variable	[°C]
b	slack variable	[°C]
c_n	slack variable	[°C]
c_p	specific heat capacity	[J/kg/K]
C_h	heat capacity of the hot stream	[W/K]
C_c	heat capacity of the cold stream	[W/K]
C_min	minimum heat capacity	[W/K]
d_n	slack variable	[-]
Δt_pr	prediction horizon	[s]
ΔT_max	maximum temperature difference	[°C]
e_n	slack variable	[-]
E_tot	total heat pump electricity use	[J]
$f(\,)$	function	[-]
$J_\mathrm{el}(t)$	electric power	[W]
k	flow coefficient	[kg/s/Pa$^{0.5}$]
$\dot{m}$	mass flow rate	[kg/s]
$\dot{m}_\mathrm{con}$	mass flow rate through the condenser	[kg/s]
mod_HP	modulation degree heat pump	[-]
$n50$	air change rate	[1/h]
N_z	number of zones	[-]
o	continuous optimisation variable	[-]
$\boldsymbol{o}$	vector of continuous optimisation variables	[-]
P_el	electric power	[W]
p	pressure	[N/m^2]
$\dot{Q}_\mathrm{con}$	condenser heat flow rate	[W]
$\dot{Q}_\mathrm{design}$	heat power design	[W]
$\dot{Q}_\mathrm{eva}$	evaporator heat flow rate	[W]
$\lvert\dot{Q}_{\mathrm{HEx},n}\rvert$	absolute heat flow rate exchanged in the n^{th} building's heat exchanger	[W]
$\dot{Q}_\mathrm{loss}$	heat losses	[W]
$\dot{Q}_{\mathrm{WSHP,con},n}$	condenser heat flow rate at the n^{th} building's heat pump	[W]
R	thermal resistance	[K/W]
t	time	[s]
t_0	initial time	[s]
$T_\mathrm{c,in}$	cold stream inlet temperature	[°C]
$T_\mathrm{c,out}$	cold stream outlet temperature	[°C]
$T_\mathrm{con,in}$	condenser inlet temperature	[°C]
$T_\mathrm{con,out}$	condenser outlet temperature	[°C]
$T_\mathrm{cold,tank}$	lower mixing volume temperature	[°C]
$T_\mathrm{eva,in}$	evaporator inlet temperature	[°C]
$T_\mathrm{eva,out}$	evaporator outlet temperature	[°C]
$T_{\mathrm{em},n}$	n^{th} zone floor surface	[°C]

	temperature	
$T_{\text{em.min}}$	minimum allowed floor surface temperature	[°C]
T_{ground}	ground temperature	[°C]
$T_{\text{h,in}}$	hot stream inlet temperature	[°C]
$T_{\text{h,out}}$	hot stream outlet temperature	[°C]
T_{in}	inlet temperature	[°C]
$T_{\text{min},n}$	n^{th} zone minimum allowed temperature	[°C]
$T_{\text{max},n}$	n^{th} zone maximum allowed temperature	[°C]
T_{mix}	mixing temperature	[°C]
T_{outlet}	outlet temperature	[°C]
$T_{\text{tank.min}}$	minimum allowed tank temperature	[°C]
$T_{\text{tank.max}}$	maximum allowed tank temperature	[°C]
$T_{\text{warm,tank}}$	upper mixing volume temperature	[°C]
$T_{\text{z},n}(t)$	n^{th} zone temperature	[°C]
T_{∞}	ambient temperature	[°C]
$\boldsymbol{u}$	vector of input variables	[-]
U	thermal transmittance value	[W/m^2/K]
V	volume	[m^3]
w	weighting factor	[W/°C^2]
x	state variable	[-]
$\boldsymbol{x}$	vector of state variables	[-]
x_0	state variable at initial time	[-]
$\boldsymbol{y}$	vector of output variables	[-]
$\boldsymbol{z}$	vector of algebraic variables	[-]

Greek letters

ϵ	Effectiveness	[-]
η	Efficiency	[-]
ρ	Density	[kg/m^3]

Abbreviations

5GDHC	Fifth Generation District Heating and Cooling
BiD	Bidirectional Energy – Directional Medium Flow
BiND	Bidirectional Energy – Non-directional Medium Flow
MPC	Model Predictive Control
NLP	Nonlinear Programming
MINLP	Mixed-integer Nonlinear Programming
WSHP	Water Source Heat Pump
HEx	Heat Exchanger
ASHP	Air Source Heat Pump
ASCH	Air Source Chiller
HVAC	Heating, Ventilation, and Air Conditioning
COP	Coefficient of Performance
EER	Energy Efficiency Ratio
SPF	Seasonal Performance Factor

REFERENCES

1. "Energy consumption in households." Accessed: Aug. 08, 2024. [Online]. Available: https://ec.europa.eu/eurostat/statistics-explained/index.php?title=Energy_consumption_in_households.
2. A. Lake, B. Rezaie, and S. Beyerlein, "Review of district heating and cooling systems for a sustainable future," Renewable and Sustainable Energy Reviews, vol. 67, pp. 417–425, Jan. 2017, https://doi.org/10.1016/j.rser.2016.09.061.
3. S. Werner, "European space cooling demands," Energy, vol. 110, pp. 148–156, Sep. 2016, https://doi.org/10.1016/j.energy.2015.11.028.
4. Y. Zhang, M. Liu, Z. O'Neill, and J. Wen, "Temperature control strategies for fifth generation district heating and cooling systems: A review and case study," Applied Energy, vol. 376, p. 124156, Dec. 2024, https://doi.org/10.1016/j.apenergy.2024.124156.
5. F. Bünning, M. Wetter, M. Fuchs, and D. Müller, "Bidirectional low temperature district energy systems with agent-based control: Performance comparison and operation optimization," Applied Energy, vol. 209, pp. 502–515, Jan. 2018, https://doi.org/10.1016/j.apenergy.2017.10.072.
6. S. Boesten, W. Ivens, S. C. Dekker, and H. Eijdems, "5th generation district heating and cooling systems as a solution for renewable urban thermal energy supply," in Advances in Geosciences, Copernicus GmbH, Sep. 2019, pp. 129–136, https://doi.org/10.5194/adgeo-49-129-2019.
7. S. S. Meibodi and F. Loveridge, "The future role of energy geostructures in fifth generation district heating and cooling networks," Energy, vol. 240, p. 122481, Feb. 2022, https://doi.org/10.1016/j.energy.2021.122481.
8. P. Mancarella, "MES (multi-energy systems): An overview of concepts and evaluation models," Energy, vol. 65, pp. 1–17, Feb. 2014, https://doi.org/10.1016/j.energy.2013.10.041.
9. S. Buffa, M. Cozzini, M. D'Antoni, M. Baratieri, and R. Fedrizzi, "5th generation district heating and cooling systems: A review of existing cases in Europe," Renewable and Sustainable Energy Reviews, vol. 104, pp. 504–522, Apr. 2019, https://doi.org/10.1016/j.rser.2018.12.059.
10. T. Sommer, M. Sulzer, M. Wetter, A. Sotnikov, S. Mennel, and C. Stettler, "The reservoir network: A new network topology for district heating and cooling," Energy, vol. 199, p. 117418, May 2020, https://doi.org/10.1016/j.energy.2020.117418.
11. E. Zanetti, D. Blum, and M. Wetter, "Control development and sizing analysis for a 5th generation district heating and cooling network using Modelica," presented at the 15th International Modelica Conference 2023, Aachen, Dec. 2023, p. 32, https://doi.org/10.3384/ecp20423.
12. H. Ahvenniemi and K. Klobut, "Future Services for District Heating Solutions in Residential Districts," [Journal of Sustainable Development of Energy, Water and Environment Systems], vol. [2], no. [2], p. [127]-[138], Jun. 2014, https://doi.org/http://dx.doi.org/10.13044/j.sdewes.2014.02.0012.
13. M. Taylor, S. Long, O. Marjanovic, and A. Parisio, "Model Predictive Control of Smart Districts With Fifth Generation Heating and Cooling Networks," IEEE Transactions on Energy Conversion, vol. 36, no. 4, pp. 2659–2669, Dec. 2021, https://doi.org/10.1109/TEC.2021.3082405.
14. P. Penttinen, J. Vimpari, K. Kontu, and S. Junnila, "How to Promote Local District Heat Production Through Real Estate Investments," J. sustain. dev. energy water environ. syst., vol. 9, no. 2, pp. 1–20, Jun. 2021, https://doi.org/10.13044/j.sdewes.d8.0343.
15. L. Frison, M. Kollmar, A. Oliva, A. Bürger, and M. Diehl, "Model predictive control of bidirectional heat transfer in prosumer-based solar district heating networks," Applied Energy, vol. 358, p. 122617, Mar. 2024, https://doi.org/10.1016/j.apenergy.2023.122617.

16. M. Wirtz, L. Neumaier, P. Remmen, and D. Müller, "Temperature control in 5th generation district heating and cooling networks: An MILP-based operation optimization," Applied Energy, vol. 288, p. 116608, Apr. 2021, https://doi.org/10.1016/j.apenergy.2021.116608.
17. M. Bilardo, F. Sandrone, G. Zanzottera, and E. Fabrizio, "Modelling a fifth-generation bidirectional low temperature district heating and cooling (5GDHC) network for nearly Zero Energy District (nZED)," Energy Reports, vol. 7, pp. 8390–8405, Nov. 2021, https://doi.org/10.1016/j.egyr.2021.04.054.
18. H. Hirsch and A. Nicolai, "An efficient numerical solution method for detailed modelling of large 5th generation district heating and cooling networks," Energy, vol. 255, p. 124485, Sep. 2022, https://doi.org/10.1016/j.energy.2022.124485.
19. J. Vivian, M. Chinello, A. Zarrella, and M. De Carli, "Investigation on Individual and Collective PV Self-Consumption for a Fifth Generation District Heating Network," Energies, vol. 15, no. 3, p. 1022, Jan. 2022, https://doi.org/10.3390/en15031022.
20. P. Saini, P. Huang, F. fiedler, A. Volkova, and X. Zhang, "Techno-economic analysis of a 5th generation district heating system using thermo-hydraulic model: A multi-objective analysis for a case study in heating dominated climate," Energy and Buildings, vol. 296, p. 113347, Oct. 2023, https://doi.org/10.1016/j.enbuild.2023.113347.
21. L. Hermans and L. Helsen, "Development of a Mixed-Integer Nonlinear Model Predictive Controller for a virtual 5th Generation District Heating and Cooling Network," presented at the IBPSA-USA SimBuild 2024, Denver, Colorado: IBPSA-USA, May 2024.
22. F. Jorissen, W. Boydens, and L. Helsen, "TACO, an automated toolchain for model predictive control of building systems: implementation and verification," Journal of Building Performance Simulation, vol. 12, no. 2, pp. 180–192, Mar. 2019, https://doi.org/10.1080/19401493.2018.1498537.
23. De Jaeger, J. Lago, and D. Saelens, "A probabilistic approach to allocate missing building parameters within district energy simulations," presented at the uSim Conference 2018, in uSim Conference, vol. 1. IBPSA Scotland, 2018, pp. 40–47. Accessed: Jul. 19, 2024. [Online]. Available: https://publications.ibpsa.org/conference/paper/?id=usim2018_004.
24. M. Wirtz, T. Schreiber, and D. Müller, "Survey of 53 Fifth‐Generation District Heating and Cooling (5GDHC) Networks in Germany," Energy Tech, vol. 10, no. 11, p. 2200749, Nov. 2022, https://doi.org/10.1002/ente.202200749.
25. F. Jorissen, G. Reynders, R. Baetens, D. Picard, D. Saelens, and L. Helsen, "Implementation and verification of the IDEAS building energy simulation library," Journal of Building Performance Simulation, vol. 11, pp. 1–20, Feb. 2018, https://doi.org/10.1080/19401493.2018.1428361.
26. F. Jorissen, "Toolchain for Optimal Control and Design of Energy Systems in Buildings," PhD Thesis, KU Leuven, Belgium, 2018.
27. ASHRAE, Handbook - Fundamentals, Atlanta, USA., 2009.
28. ANSI/ASHRAE, Standard 55 - 2004: Thermal Environmental Conditions for Human Occupancy, Atlanta, USA., 2004.
29. International Organization for Standardization, ISO 7730:2005, Ergonomics of the thermal environment: Analytical determination and interpretation of thermal comfort using calculation of the PMV and PPD indices and local thermal comfort criteria., 2005.
30. C. Verhelst, "Model Predictive Control of Ground Coupled Heat Pump Systems for Office Buildings," PhD Thesis, KU Leuven, Belgium, 2012.
31. D. Picard, F. Jorissen, and L. Helsen, "Methodology for Obtaining Linear State Space Building Energy Simulation Models," presented at the The 11th International Modelica Conference, Sep. 2015, pp. 51–58, https://doi.org/10.3384/ecp1511851.
32. M. Wetter, "Fan And Pump Model That Has A Unique Solution For Any Pressure Boundary Condition And Control Signal," presented at the Building Simulation 2013, in

Building Simulation, vol. 13. IBPSA, 2013, pp. 3505–3512, https://doi.org/10.26868/25222708.2013.1040.
33. Koschenz, M., Lehmann, B., "Thermoactive component systems tabs" (In German, "Thermoaktive Bauteilsysteme tabs"), EMPA, Duebendorf Switzerland, ISBN 3-905594-19-6, 2000.

APPENDIX

The most fundamental energy equations (among which conservation of energy) of the components in the analysed thermal systems are reported in **Table 4**. A more detailed and complete formulation of all equations of the component models can be found in the code and documentation of the IDEAS and Buildings library and in the PhD text of F. Jorissen [26].

The high-order white-box building envelope models from IDEAS library include several heat transfer effects (one-dimensional conduction, convection, short and longwave radiation), some of which are intrinsically nonlinear. Picard *et al.* [31] developed a methodology to linearise the initial IDEAS building envelope model equations, resulting in a state-space representation in eqs. (5) and (6), where $\boldsymbol{x}$ represents the state vector, $\boldsymbol{u}$ includes the model inputs (boundary conditions and HVAC equations), and $\boldsymbol{y}$ denotes the model's output variables. The matrices A, B, C and D are constants derived from the linearisation of the building envelope equations:

$$\frac{d\boldsymbol{x}(t)}{dt} = A\boldsymbol{x}(t) + C\boldsymbol{u}\big(t, \boldsymbol{x}(t)\big) \tag{5}$$

$$\boldsymbol{y}(t) = C\boldsymbol{x}(t) + D\boldsymbol{u}\big(t, \boldsymbol{x}(t)\big) \tag{6}$$

In all thermal system components conservation of mass is applied. The momentum equations are implemented using a flow coefficient determined at nominal flow conditions, as follows:

$$\dot{m}(t) = k\sqrt{\Delta p(t)}, \quad k = \frac{\dot{m}_{\text{nom}}}{\sqrt{\Delta p_{\text{nom}}}} \tag{7}$$

Table 4. Overview of fundamental energy equations of thermal models

Component	Fundamental energy equation
Building envelope [31][26]	$\frac{d\boldsymbol{x}(t)}{dt} = A\boldsymbol{x}(t) + C\boldsymbol{u}\big(t, \boldsymbol{x}(t)\big)$ $\boldsymbol{y}(t) = C\boldsymbol{x}(t) + D\boldsymbol{u}\big(t, \boldsymbol{x}(t)\big)$
Circulation pump[26][32]	$P_{\text{el}}(t) = \frac{\Delta p(t)\dot{m}(t)}{\rho\eta}$
Embedded system [33]	$\dot{Q}(t) = \dot{m}(t)c_p\big(T_{\text{out}}(t) - T_{\text{in}}(t)\big) = \frac{T_{\text{out}}(t) - T_{\text{in}}(t)}{R(t)}$ $R(t) = f(\dot{m}(t)$, floor properties, pipe spacing$)$
Heat exchanger	$\dot{Q}(t) = C_{\text{c}}(t)\left(T_{\text{c,out}}(t) - T_{\text{c,in}}(t)\right) = C_{\text{h}}(t)\left(T_{\text{c,out}}(t) - T_{\text{c,in}}(t)\right)$ $\dot{Q}(t) = \epsilon C_{\min}\left(T_{\text{h,in}}(t) - T_{\text{c,in}}(t)\right)$
Heat pump [26]	$\dot{Q}_{\text{con}}(t) = mod_{\text{HP}}\dot{m}_{\text{con}}(t)c_p\Delta T_{\max} = \dot{m}_{\text{con}}(t)c_p(T_{\text{con,out}} - T_{\text{con,in}})$ $\dot{Q}_{\text{eva}}(t) = \dot{m}_{\text{eva}}(t)c_p(T_{\text{eva,out}} - T_{\text{eva,in}})$

	$P_{\mathrm{el}} = \dfrac{\dot{Q}_{\mathrm{con}}}{\mathrm{COP}}$
Pipe	$T_{\mathrm{out}}(t) = T_{\mathrm{mix}}(t)$ $\dot{Q}_{\mathrm{loss}}(t) = \dot{m}(t) c_p \left(T_{\mathrm{in}}(t) - T_{\mathrm{mix}}(t)\right)$ $= \dfrac{T_{\mathrm{mix}}(t) - T_{\mathrm{ground}}(t)}{R_{\mathrm{pipe}}}$
Mixing volume	$\rho c_p V \dfrac{dT_{\mathrm{mix}}(t)}{dt} = \sum_{\mathrm{in}} \dot{m}(t) c_p T_{\mathrm{mix}}(t)$ $- \sum_{\mathrm{out}} \dot{m}(t) c_p T_{\mathrm{mix}}(t)$ $- \dfrac{T_{\mathrm{mix}}(t) - T_{\infty}(t)}{R}$

Paper submitted: 02.01.2025
Paper revised: 30.03.2025
Paper accepted: 31.03.2025